THE JOURNAL OF PHYSICAL CHEMISTRY LETTERS
A JOURNAL OF THE AMERICAN CHEMICAL SOCIETY

pubs.acs.org/JPCL

Letter

Control of Reversible Oxidative Addition/Reductive Elimination of Surface-Attached Catalysts by External Electric Fields

Zhuoran Long,[▽] H. Ray Kelly,[▽] Pablo E. Videla, Jan Paul Menzel, Tianquan Lian, Clifford P. Kubiak, and Victor S. Batista*

Cite This: *J. Phys. Chem. Lett.* 2025, 16, 2881−2886

Read Online

ACCESS | Metrics & More | Article Recommendations | Supporting Information

ABSTRACT: We demonstrate that applied electric fields at interfaces can control the oxidative addition/reductive elimination equilibria of surface-attached molecular catalysts without any synthetic modification. Density functional theory (DFT) calculations show that the oxidative addition of HCl to a Co complex is "field switchable", being favorable under negative fields but unfavorable under sufficiently positive fields. Extending the analysis to different substrates (O_2, H_2) and metal centers (Rh, Ir) reveals consistent trends in the magnitude of the electric field effect: Co > Rh ≈ Ir and HCl > O_2 > H_2. Our analysis indicates that these field-dependent effects are driven by changes in the permanent dipole moment, offering key insights for the design of field-controllable catalytic systems. This framework presents a novel strategy to overcome the "Goldilocks problem" of balancing competing catalytic steps by leveraging applied electric fields to dynamically tune catalytic reactivity in situ.

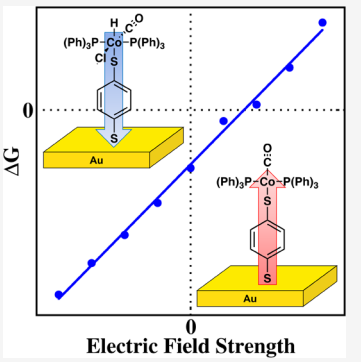

Oxidative addition and reductive elimination are two of the most essential mechanistic steps in transition metal catalysis, and play a role in a wide range of important reactions including cross-coupling reactions and industrial processes for acetic acid production.[1−10] Optimizing catalytic activity has traditionally relied on extensive synthetic efforts to design ligands of metal catalysts that facilitate both of these microscopic processes efficiently. These efforts often involve modifying the electron donor or acceptor character of the ligands: electron-donating ligands increase the electron density at the metal center, promoting oxidative addition, while electron-withdrawing ligands decrease the electron density at the metal center, enhancing reductive elimination. However, this creates a "Goldilocks problem", where both steps must be delicately balanced against each other to sustain catalysis. For instance, the activation of strong bonds such as C−F may require highly electron-rich metal centers, rendering oxidative addition effectively irreversible,[11] hindering the development of efficient catalysts for challenging chemical reactions.

In this work, we present an alternative strategy to bypass the Goldilocks problem by leveraging an applied interfacial electric field (bias) to dynamically control the direction of oxidative addition and reductive elimination reactions. Electric fields are known to influence catalytic activity and selectivity: internal electric fields play a key role in enzyme catalysis,[12−17] and external fields have been shown to accelerate reactions such as the Diels−Alder cycloaddition.[18,19] In the area of heterogenized catalysis, attaching molecular complexes to electrode surfaces enables orientation-dependent control of reactivity by the electric field.[20] For example, Heo et al. utilized fields to control the properties of surface-bound reactants for cross-coupling reactions,[21] while Gorin et al. modulated the selectivity of a surface-attached Rh porphyrin catalyst.[22] Our previous computational studies further demonstrated field-dependent hydricity shifts in Cp*Ir-bipyridine and Cp*Ir-phenylpyridine on Au surfaces.[23] Building on these advances, we explore how applied electric fields can tune catalytic behavior, offering a dynamic and versatile solution for overcoming challenges in catalytic design.

In this work, we use analogues of the well-studied Vaska's complex[24−26] attached to Au surfaces to computationally investigate the effect of external fields on oxidative addition and reductive elimination. Shaik and co-workers previously studied the effect of external fields on the oxidative addition of alkyl and aryl electrophiles to palladium catalysts.[27] Here, we explore the possibility of reversibly switching oxidative addition and reductive elimination (Figure 1). We address the impact of surface attachment, the effect of different metal centers, and the potential for spectroscopic characterization.

In the following content, we will demonstrate the field switchability for a Vaska's complex analogue with a cobalt center (noted as **Co**, see Figure 1 and Figure 2A) attached to a gold electrode surface. This system undergoes oxidative addition of

Received: January 22, 2025
Revised: March 3, 2025
Accepted: March 5, 2025

https://doi.org/10.1021/acs.jpclett.5c00215
J. Phys. Chem. Lett. 2025, 16, 2881−2886

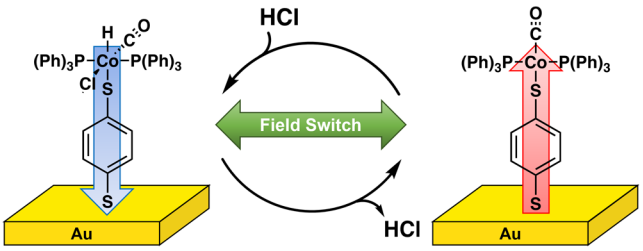

Figure 1. Surface-attached Co complexes (**Co**, on the left) undergo oxidative addition of HCl when a negative field (blue downward arrow) is applied. Conversely, HCl is reductively eliminated from the HCl adduct (**Co**-HCl, on the right) when a positive field (red upward arrow) is applied.

HCl under negative field (bias) and reductively eliminates it under sufficiently positive field (bias). The effect of applied electric fields on the thermodynamics of this reaction is compared to those on analogous oxidative addition reactions with different metal centers (Rh, Ir, noted as **Rh** and **Ir**, respectively) and substrates (O_2, H_2). This approach provides insights into the field-dependent modulation of catalytic reactivity across diverse systems.

Density functional theory (DFT) calculations were performed to evaluate the impact of applied electric fields on a series of oxidative addition/reductive elimination equilibria. All calculations were performed with the Gaussian 16, rev. C.01 package[28] employing the PBE functional[29] with Grimme's D3 dispersion correction with Becke–Johnson damping.[30,31] Geometry optimizations and frequency calculations were carried out in the gas phase, utilizing the LANL2DZ basis set and pseudopotential for Au atoms,[32] the Def2SVP basis set for Co, Rh or Ir atoms (with corresponding pseudopotential for Rh and Ir),[33] and the 6-31G(d,p) basis set for nonmetal atoms.[34,35] To reduce errors caused by low-frequency modes, thermodynamic corrections were calculated with quasi-harmonic frequency analysis using the Goodvibes code,[36] with entropy corrections via the Grimme method[37] and enthalpy corrections via the Head–Gordon method.[38] The frequency cutoff was set to 100 cm^{-1}. Single point calculations of electronic energy on the optimized geometries employed the Def2SVP basis set and pseudopotential on Au atoms, Def2TZVP basis on Co, Rh or Ir atom with corresponding pseudopotential on Rh or Ir,[33] and the 6-311+G(2df,p) basis set on nonmetals,[39,40] in the Polarizable Continuum Model (PCM) implicit solvent of dichloromethane.[41] This level of theory was chosen based on a previous study which benchmarked DFT calculations of Gibbs free energy for 11 diverse Ir-catalyzed reactions against experimental data.[42] Additional polarization functions were incorporated to the selected basis sets to better account for the influence of applied electric field on the metal center. Counterpoise corrections were applied to calculations of adducts in the gas phase using the same basis sets and pseudopotentials as in the single-point calculations. The Au(111) electrode surface was modeled as a single layer of gold atoms in the *xy*-plane as described in detail in our previous work.[23] All Au atoms were frozen during the geometry optimization. An external electric field perpendicular to this surface (along the *z*-axis) was applied. All visualizations were created using GaussView Version 6.0.16.[43] Snapshots of the optimized geometries are provided in Figure 2A and Figures S1–S3. The axes are shown in Figure 2A and Figure S1.

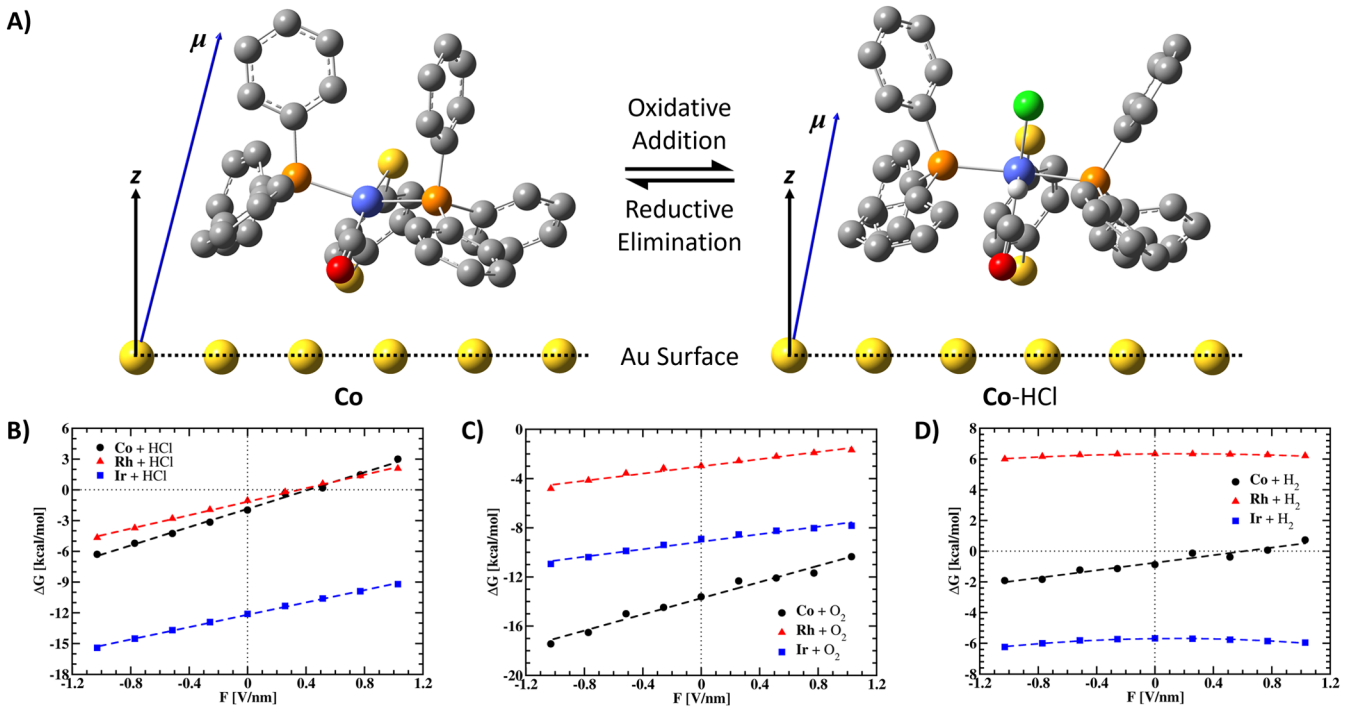

Figure 2. (A) Snapshots of **Co** and **Co**-HCl complexes. The dipole moments (μ) are represented as blue arrows with lengths proportional to their magnitudes. Carbon-bound hydrogens are omitted for clarity. The color scheme is as follows: H (white), C (gray), O (red), P (orange), S (yellow), Co (blue), Au (yellow), and Cl (green). Au surfaces (black dotted lines) lie in the *xy*-plane. The *z*-axes are indicated by black arrows. Free energy changes (ΔG) for the oxidative addition of (B) HCl, (C) O_2, and (D) H_2 to **Co** (black circle), **Rh** (red triangle) and **Ir** (blue square) as a function of applied field strength. Dashed lines represent linear fits. Negative free energy changes ($\Delta G < 0$) indicate that oxidative addition is thermodynamically favored, while positive free energy changes ($\Delta G > 0$) indicate that the reductive elimination is favored.

https://doi.org/10.1021/acs.jpclett.5c00215
J. Phys. Chem. Lett. 2025, 16, 2881–2886

Table 1. Changes in the *z*-Component of the Permanent Dipole Moment ($\Delta\mu_z$) for the Addition of HCl, O_2, and H_2 to Co, Rh, and Ir compared with free energy response to the applied electric field ($\Delta G/F$)[a]

metal	substrate	$\Delta\mu_z$ [kcal mol^{-1}/(V nm^{-1})]	$\Delta G/F$ [kcal mol^{-1}/(V nm^{-1})]	fitted zero-field ΔG [kcal mol^{-1}]	R^2
Co	HCl	−4.3	+4.5	−1.9	0.9957
	O_2	−3.1	+3.3	−13.7	0.9788
	H_2	−1.0	+1.2	−0.8	0.9519
Rh	HCl	−3.1	+3.3	−1.2	0.9983
	O_2	−1.5	+1.5	−3.0	0.9751
	H_2	0.0	nonlinear[b]	(+6.3)	(0.9663)
Ir	HCl	−2.8	+3.0	−12.2	0.9986
	O_2	−1.2	+1.5	−9.1	0.9728
	H_2	+0.1	nonlinear[c]	(−5.7)	(0.9786)

[a]The table also includes $\Delta G/F$ (slopes), fitted zero-field ΔG (intercepts), and R^2 (coefficients of determination) for the best-fit lines for reaction free energy change (ΔG) *vs.* field strength (F). For the two nonlinear cases (H_2 addition to **Rh** and **Ir**), ΔG at 0 V nm^{-1} and R^2 are provided in parentheses. [b]$\Delta G = -0.22F^2 + 0.08F + 6.34$. [c]$\Delta G = -0.39F^2 + 0.11F - 5.69$.

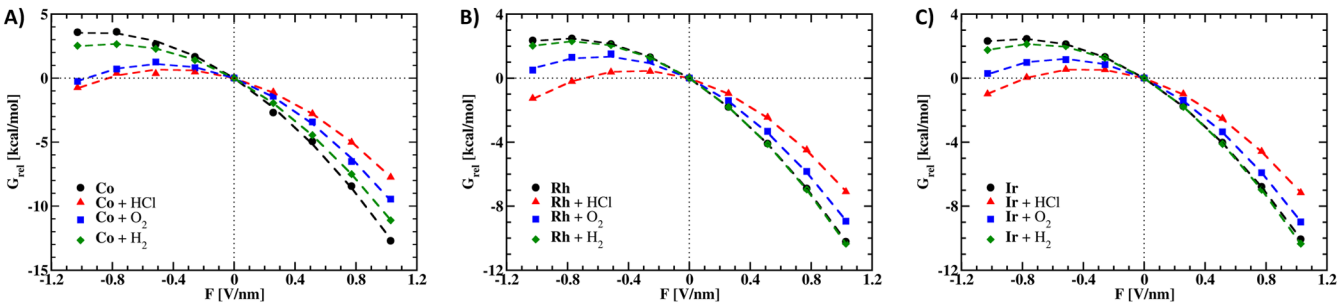

Figure 3. Relative free energy of **Co** (black circle) and its corresponding HCl (red trangle), O_2 (blue square), and H_2 (green diamond) adducts as an external field is applied. The dashed lines are the best quadratic fits.

External electric fields were applied across a range of field strengths, approximately ±1 V nm^{-1}, consistent with typical interfacial electrode fields in the Helmholtz layer of an electrode.[14,44−46] Experimental characterization of such fields at electrochemical interfaces is often performed using Stark effect spectroscopy, where shifts in vibrational frequencies induced by the field provide a measure of field strength. For this technique to be effective, the vibrational mode must strongly interact with the applied field, which occurs when the transition dipole is parallel to the field. Geometry optimizations of the **Co** (Figure 2A, left) and its HCl adduct (**Co**-HCl, Figure 2A, right) at zero field on an Au(111) surface predict that the carbonyl ligand (CO) orients toward the surface. In the case of **Co**, the plane containing the metal center (as defined by the P and S atoms) forms a 21° angle with the surface, while for for the **Co**-HCl adduct, this angle is 24°. The CO group of **Co** is oriented at a 46° angle relative to the *z*-axis, which changes to 12° upon oxidative addition of HCl. This adjustment increases the alignment of the transition dipole with the applied field, enhancing the Stark shift.

Due to differences in CO orientation, **Co** and its HCl adduct exhibit distinct CO Stark shifts in our DFT calculations (Figure S4). **Co**, along with **Rh** and **Ir**, displays a quadratic Stark shift, while the **Co**-HCl adduct exhibits a linear Stark shift (−4.0 cm^{-1}/(V nm^{-1})), which enables direct measurement of field strength. These differences highlight the role of molecular geometry in dictating field-induced vibrational behavior.

Figure 2B shows that the oxidative addition of HCl to **Co** is spontaneous at zero field, with a reaction free energy change of ΔG = −1.9 kcal mol^{-1}. Negative fields further facilitate the oxidative addition ($\Delta G < 0$), while positive fields promote reductive elimination ($\Delta G > 0$). Across the applied field range, a reaction free energy span exceeding 9 kcal mol^{-1} was accessed over the range of applied fields. The response of ΔG to field strength (F) was linear, with a field-tuning rate of 4.5 kcal mol^{-1}/(V·nm^{-1}). This tunning rate closely aligns with the calculated zero-field dipole moment change ($\Delta\mu_z$) associated with the oxidative addiction reaction ($\Delta\mu_z$(**Co**) = μ_z(**Co**-HCl) − μ_z(**Co**), see Table 1). This correlation suggests that the field switchability primarily arises from differential stabilization or destabilization of reactants and products, driven by the interaction between the electric field and the permanent dipole moment of the surface-attached catalytic complex.

Vaska's complex analogues with other metal centers (Rh, Ir) and substrates (O_2, H_2) were also investigated to establish general design rules for field-responsive catalytic systems. A clear trend was observed in which smaller metal centers were more affected by the applied electric field than larger metals, following the order Co > Rh ≈ Ir, as indicated by the slope of the ΔG vs field strength curves (Figure 2 and Table 1).

The oxidative addition/reductive elimination of HCl was significantly more influenced by the field compared to O_2, while only minor effects were observed for H_2. Notably, the field was able to invert the reaction equilibrium for HCl addition to both **Co** and **Rh**. In contrast, the reaction free energy for HCl oxidative addition to **Ir** at zero field was so favorable that equilibrium inversion was not achieved within the tested range of field strength.

These results suggest that field-switchable behavior is more pronounced for reactions near thermodynamic equilibrium in

https://doi.org/10.1021/acs.jpclett.5c00215
J. Phys. Chem. Lett. 2025, 16, 2881−2886

Table 2. Fitted Parameters ($G_{rel} = aF^2 + bF$) and Coefficients of Determination (R^2) of Best Fit for Relative Free Energy (G_{Rel}) vs Applied Field Strength compared with half of the polarizability zz-components ($\frac{1}{2}\alpha_{zz}$) and dipole moment z components (μ_z)

complex	a [kcal^2 mol^{-2}/(V^2 nm^{-2})]	b [kcal mol^{-1}/(V nm^{-1})]	$\frac{1}{2}\alpha_{zz}$[kcal^2 mol^{-2}/(V^2 nm^{-2})]	μ_z [kcal mol^{-1}/(V nm^{-1})]	R^2
Co	−4.27	−7.83	3.6	7.8	0.9988
Co-HCl	−4.02	−3.37	3.8	3.5	0.9979
Co-O_2	−4.64	−4.54	4.1	4.7	0.9988
Co-H_2	−4.07	−6.60	3.7	6.8	1.0000
Rh	−3.72	−6.09	3.4	6.0	1.0000
Rh-HCl	−3.96	−2.80	3.5	3.0	0.9999
Rh-O_2	−3.92	−4.63	4.0	4.5	0.9994
Rh-H_2	−3.93	−6.01	3.5	6.1	1.0000
Ir	−3.66	−6.01	3.3	6.0	1.0000
Ir-HCl	−3.84	−3.00	3.5	3.2	1.0000
Ir-O_2	−4.12	−4.48	4.0	4.8	0.9999
Ir-H_2	−4.07	−5.90	3.5	6.0	1.0000

the absence of an electric field. Under these conditions, small changes in the field strength can alter the equilibrium, shifting the favored species on the surface and enabling dynamic control over catalytic activity.

To analyze the linear relation between the reaction free-energy change (ΔG) and external electric field strength (F), we plotted the relative free energy ($G_{rel} = G_F - G_0$) for each individual species, as shown in Figure 3. The relative free energy follows a quadratic correlation with the field strength:

$$G_{rel} = aF^2 + bF \quad (1)$$

This behavior can be compared to the effect of a homogeneous field (F) applied along the z-axis on the molecule potential energy (U), described by the following equation:

$$U_F = U_0 - \mu_Z F - \frac{1}{2}\alpha_{zz}F^2 \quad (2)$$

Here, U_0 represents the zero-field potential energy of the molecule, μ_Z is the z-component of the zero-field dipole moment, and α_{zz} is the zz-component of the polarizability tensor. Positive fields are defined as pointing away from positive charges. Higher-order polarizabilities, as well as field-induced molecular reorientations and conformation changes, are neglected for simplicity.

As summarized in Table 2, the fitted coefficients of G_{rel} closely align with DFT-calculated molecule properties (a vs $\frac{1}{2}\alpha_{zz}$ and b vs μ_z). The quadratic term primarily arises from the interaction between the electric field and the zz-component of the molecule polarizability (α_{zz}), reflecting the electron-donating (negative field) or electron-withdrawing (positive field) effects. The similarity in quadratic coefficients a (and also $\frac{1}{2}\alpha_{zz}$) between the reactants (Vaska's complex analogues **Co**, **Ir**, or **Rh**) and their products (HCl/O_2/H_2 adducts) cancels out when calculating the reaction free-energy change (ΔG). This explains the linear dependence of the reaction ΔG on the external electric field strength (F). This cancellation indicates that the field-induced electron-donating or withdrawing effects are comparable between the reactants and products and, therefore, do not contribute to the electric field effects observed in this study. Instead, the linear term arises from the alignment between the electric field and the (z-component of the) molecular permanent dipole moment (μ_z). When a positive electric field aligns parallel to the dipole moment of the complex, it stabilizes the reactants more than the products, promoting reductive elimination. Conversely, when a negative field aligns antiparallel to the dipole moment, it destabilizes the reactants more than the products, promoting oxidative addition.

The data in Table 2 also explains the observed trend of field-tuning rates for different metal centers (Co > Rh ≈ Ir). Adducts of the same substrates exhibit similar (z-components of) dipole moments across different metal centers, while the (z-components of) dipole moments of the reactants follow the trend Co > Rh ≈ Ir. A similar pattern is observed for the total dipole moments, as listed in Table S1. These findings indicate that the variation in tuning rates among metal centers is determined by the differences in the dipole moments of the reactants.

The differences in dipole moments for the Vaska's complex analogues can be interpreted using the Hard and Soft Acids and Bases (HSAB) theory. Co, as a harder acid compared to Rh and Ir, interacts with the soft bases S (from the benzene-1,4-dithiolate ligand) and P (from the triphenylphosphine ligands) in a more ionic and less covalent manner. This results in Co being more positively charged than Rh and Ir. Additionally, due to the position of the metal center in the complex (higher along the positive z-axis than other atoms in the complex), this increased positive charge leads to stronger charge separation and a larger (z-component of the) dipole moment for **Co** compared to **Rh** and **Ir**.

The trend in field-tuning rates by for substrates (HCl > O_2 > H_2) can be explained by two primary factors: (a) the internal dipole moments of the substrate moieties, and (b) charge redistribution during oxidative addition and bond formation with the metal center:

(a) **Substrate Dipole Moments**: The heteronuclear diatomic molecule HCl possesses a significant permanent dipole moment (1.8 kcal mol^{-1}/(V nm^{-1}), as computed in dichloromethane. In the **Co**-HCl adduct, the H and Cl moiety aligns approximately 9° off the z-axis, nearly antiparallel to the dipole moment of **Co** and the **Co**-HCl adduct. Upon oxidative addition of HCl, the dipole moment of HCl is effectively added to the dipole moment of the adduct. This results in a larger decrease of (the z-component of) the dipole moment and leads to a higher tunning rate for HCl compared to O_2 and H_2.

(b) **Charge Redistribution:** Oxidative addition redistributes charge by decreasing the electron density on the metal center (oxidation) and increasing the charge density on the substrate moieties (reduction). The added negative

https://doi.org/10.1021/acs.jpclett.5c00215
J. Phys. Chem. Lett. 2025, 16, 2881−2886

charge centers (Cl, O, or H) are positioned along the positive *z*-axis relative to the metal center, reducing the z-component of the dipole moments in all adducts. Cl and O, being more electronegativity than H, induce greater charge redistribution. Additionally, Cl and O have longer bond distances with the metal center, amplifying the reduction in the z-component of the dipole moment during oxidative addition. Consequently, substrates with more electronegative atoms and longer bond distances, such as HCl and O_2, exhibit higher field-tuning rates compared to H_2.

In summary, we have demonstrated that external electric fields can effectively control oxidative addition/reductive elimination equilibria, using the model reaction of HCl addition to Vaska's complex analogues **Co** and **Rh**. This novel approach allows for the manipulating of slow catalytic steps through the application of an electric field in situ, without requiring chemical modifications. Furthermore, it opens the intriguing possibility of employing alternating fields to dynamically lower the barriers of key catalytic steps, thereby driving the system through the catalytic cycle. This strategy shifts the focus of catalyst design toward optimizing factors such as selectivity, rather than balancing competing reverse steps.

Importantly, this approach offers a non-Faradaic mechanism for introducing electric energy into chemical reactions, where the catalyst acts as a device that converts electric energy into chemical energy. Our findings reveal that changes in the permanent dipole moment of catalytic complexes are the dominating factor behind this field-switchability. A critical design criterion for new systems is ensuring that the oxidative addition/reductive elimination equilibrium is close to thermodynamic balance ($\Delta G \approx 0$) so that the reaction direction can be reversibly switched within an accessible range of field strength.

We also found that smaller metal centers are more susceptible to control by electric fields. Their bonds with ligands are more ionic in nature, and therefore, these complexes exhibit greater charge separation, making them more susceptibility to dipole-induced changes. Reactions involving polar substrates or target bonds containing high electronegative elements show higher field-tuning rates that those with nonpolar substrates containing only C and H. These insights provide useful guidelines for designing catalysts for practical applications.

Beyond providing a potential method for addressing the "Goldilocks" problem of balancing the reactivity of two competing microscopic reverse steps in a catalytic cycle, this approach also enables precise in situ control of reaction progress. For example, stopping at intermediate stages of catalytic cycles could aid in isolating intermediates for mechanistic studies or enable the design of stepwise catalytic processes via temporal or spatial separation of catalytic steps. Moreover, this method has the potential to improve selectivity by stabilizing or destabilizing specific transition states or intermediates with significantly different dipole moments, enhancing control over reaction pathways.

■ ASSOCIATED CONTENT

Supporting Information

The Supporting Information is available free of charge at https://pubs.acs.org/doi/10.1021/acs.jpclett.5c00215.

Snapshots of model systems used for computation. Stark shifts of the C−O stretching mode frequency. Isotropic polarizability and total dipole moment (PDF)

■ AUTHOR INFORMATION

Corresponding Author

Victor S. Batista − *Department of Chemistry, Yale University, New Haven, Connecticut 06520-8107, United States; Energy Science Institute, Yale University, West Haven, Connecticut 06516, United States;* orcid.org/0000-0002-3262-1237; Email: victor.batista@yale.edu

Authors

Zhuoran Long − *Department of Chemistry, Yale University, New Haven, Connecticut 06520-8107, United States; Energy Science Institute, Yale University, West Haven, Connecticut 06516, United States;* orcid.org/0000-0002-2957-9568

H. Ray Kelly − *Department of Chemistry, Yale University, New Haven, Connecticut 06520-8107, United States; Energy Science Institute, Yale University, West Haven, Connecticut 06516, United States;* orcid.org/0000-0003-3811-0662

Pablo E. Videla − *Department of Chemistry, Yale University, New Haven, Connecticut 06520-8107, United States; Energy Science Institute, Yale University, West Haven, Connecticut 06516, United States;* orcid.org/0000-0003-0742-0342

Jan Paul Menzel − *Department of Chemistry, Yale University, New Haven, Connecticut 06520-8107, United States; Energy Science Institute, Yale University, West Haven, Connecticut 06516, United States;* orcid.org/0000-0002-1312-5000

Tianquan Lian − *Department of Chemistry, Emory University, Atlanta, Georgia 30322, United States;* orcid.org/0000-0002-8351-3690

Clifford P. Kubiak − *Department of Chemistry and Biochemistry, University of California, San Diego, La Jolla, California 92093, United States;* orcid.org/0000-0003-2186-488X

Complete contact information is available at: https://pubs.acs.org/10.1021/acs.jpclett.5c00215

Author Contributions

▽Authors Z. Long and H. R. Kelly contributed equally to this work.

Notes

The authors declare no competing financial interest.

■ ACKNOWLEDGMENTS

V.S.B. acknowledges financial support from the United States Army Research Office (Award No. W911NF2110337). T.L. acknowledges the support by the Air Force Office of Scientific Research (AFOSR), under AFOSR Award No. FA9550-18-1-0420. C.P.K. acknowledges support by National Science Foundation (NSF) (Nos. CHE-1853908 and CHE-2153757). Any opinions, findings, and conclusions or recommendations expressed in this material are those of the author(s) and do not necessarily reflect the views of the National Science Foundation.

■ REFERENCES

(1) Labinger, J. A. Tutorial on Oxidative Addition. *Organometallics* **2015**, *34* (20), 4784−4795.

(2) Halpern, J. Oxidative-addition reactions of transition metal complexes. *Acc. Chem. Res.* **1970**, *3* (11), 386−392.

(3) Zeni, G.; Larock, R. C. Synthesis of Heterocycles via Palladium-Catalyzed Oxidative Addition. *Chem. Rev.* **2006**, *106* (11), 4644−4680.

(4) Baudoin, O. Transition metal-catalyzed arylation of unactivated C(sp3)−H bonds. *Chem. Soc. Rev.* **2011**, *40* (10), 4902−4911.

(5) Jana, R.; Pathak, T. P.; Sigman, M. S. Advances in Transition Metal (Pd,Ni,Fe)-Catalyzed Cross-Coupling Reactions Using Alkyl-organometallics as Reaction Partners. *Chem. Rev.* **2011**, *111* (3), 1417−1492.
(6) Dyker, G. Transition Metal Catalyzed Coupling Reactions under C−H Activation. *Angew. Chem., Int. Ed.* **1999**, *38* (12), 1698−1712.
(7) He, C. Oxidative Coupling Reactions Between Hydrocarbons and Organometallic Reagents (The Second Generation). In *Transition Metal Catalyzed Oxidative Cross-Coupling Reactions*; Lei, A., Ed.; Springer: Berlin, Heidelberg, 2019; pp 41−98.
(8) Souillart, L.; Cramer, N. Catalytic C−C Bond Activations via Oxidative Addition to Transition Metals. *Chem. Rev.* **2015**, *115* (17), 9410−9464.
(9) Paulik, F. E.; Roth, J. F. Novel catalysts for the low-pressure carbonylation of methanol to acetic acid. *Chem. Commun. (London)* **1968**, No. 24, 1578a−1578a.
(10) Sunley, G. J.; Watson, D. J. High productivity methanol carbonylation catalysis using iridium: The Cativa process for the manufacture of acetic acid. *Catal. Today* **2000**, *58* (4), 293−307.
(11) Garg, A.; Haswell, A.; Hopkinson, M. N. C−F Bond Insertion: An Emerging Strategy for Constructing Fluorinated Molecules. *Chem.—Eur. J.* **2024**, *30* (20), e202304229.
(12) Fried, S. D.; Bagchi, S.; Boxer, S. G. Extreme electric fields power catalysis in the active site of ketosteroid isomerase. *Science* **2014**, *346* (6216), 1510−1514.
(13) Fried, S. D.; Boxer, S. G. Electric Fields and Enzyme Catalysis. *Annu. Rev. Biochem.* **2017**, *86*, 387−415.
(14) Bhattacharyya, D.; Videla, P. E.; Palasz, J. M.; Tangen, I.; Meng, J.; Kubiak, C. P.; Batista, V. S.; Lian, T. Sub-Nanometer Mapping of the Interfacial Electric Field Profile Using a Vibrational Stark Shift Ruler. *J. Am. Chem. Soc.* **2022**, *144* (31), 14330−14338.
(15) Shaik, S.; Mandal, D.; Ramanan, R. Oriented electric fields as future smart reagents in chemistry. *Nat. Chem.* **2016**, *8* (12), 1091−1098.
(16) Che, F.; Gray, J. T.; Ha, S.; Kruse, N.; Scott, S. L.; McEwen, J.-S. Elucidating the Roles of Electric Fields in Catalysis: A Perspective. *ACS Catal.* **2018**, *8* (6), 5153−5174.
(17) Léonard, N. G.; Dhaoui, R.; Chantarojsiri, T.; Yang, J. Y. Electric Fields in Catalysis: From Enzymes to Molecular Catalysts. *ACS Catal.* **2021**, *11* (17), 10923−10932.
(18) Meir, R.; Chen, H.; Lai, W.; Shaik, S. Oriented Electric Fields Accelerate Diels−Alder Reactions and Control the endo/exo Selectivity. *ChemPhysChem* **2010**, *11* (1), 301−310.
(19) Aragonès, A. C.; Haworth, N. L.; Darwish, N.; Ciampi, S.; Bloomfield, N. J.; Wallace, G. G.; Diez-Perez, I.; Coote, M. L. Electrostatic catalysis of a Diels−Alder reaction. *Nature* **2016**, *531* (7592), 88−91.
(20) Long, Z.; Meng, J.; Weddle, L. R.; Videla, P. E.; Menzel, J. P.; Cabral, D. G. A.; Liu, J.; Qiu, T.; Palasz, J. M.; Bhattacharyya, D.; et al. The Impact of Electric Fields on Processes at Electrode Interfaces. *Chem. Rev.* **2025**, *125* (3), 1604−1628.
(21) Heo, J.; Ahn, H.; Won, J.; Son, J. G.; Shon, H. K.; Lee, T. G.; Han, S. W.; Baik, M.-H. Electro-inductive effect: Electrodes as functional groups with tunable electronic properties. *Science* **2020**, *370* (6513), 214−219.
(22) Gorin, C. F.; Beh, E. S.; Bui, Q. M.; Dick, G. R.; Kanan, M. W. Interfacial Electric Field Effects on a Carbene Reaction Catalyzed by Rh Porphyrins. *J. Am. Chem. Soc.* **2013**, *135* (30), 11257−11265.
(23) Kelly, H. R.; Videla, P. E.; Kubiak, C. P.; Lian, T.; Batista, V. S. Controlling Hydricity of Adsorbed Catalysts with Applied Electric Fields. *J. Phys. Chem. C* **2023**, *127* (14), 6733−6743.
(24) Vaska, L.; DiLuzio, J. W. Carbonyl and Hydrido-Carbonyl Complexes of Iridium by Reaction with Alcohols. Hydrido Complexes by Reaction with Acid. *J. Am. Chem. Soc.* **1961**, *83* (12), 2784−2785.
(25) Vaska, L. Oxygen-Carrying Properties of a Simple Synthetic System. *Science* **1963**, *140* (3568), 809.
(26) Ugo, R.; Pasini, A.; Fusi, A.; Cenini, S. Kinetic investigation of some electronic and steric factors in oxidative addition reactions to Vaska's compound. *J. Am. Chem. Soc.* **1972**, *94* (21), 7364−7370.
(27) Joy, J.; Stuyver, T.; Shaik, S. Oriented External Electric Fields and Ionic Additives Elicit Catalysis and Mechanistic Crossover in Oxidative Addition Reactions. *J. Am. Chem. Soc.* **2020**, *142* (8), 3836−3850.
(28) *Gaussian 16, Rev. C.01*; Gaussian: Wallingford, CT, 2016. (Accessed July 17, 2024.)
(29) Perdew, J. P.; Burke, K.; Ernzerhof, M. Generalized Gradient Approximation Made Simple. *Phys. Rev. Lett.* **1996**, *77* (18), 3865−3868.
(30) Grimme, S.; Antony, J.; Ehrlich, S.; Krieg, H. A consistent and accurate ab initio parametrization of density functional dispersion correction (DFT-D) for the 94 elements H-Pu. *J. Chem. Phys.* **2010**, *132* (15). DOI: 10.1063/1.3382344.
(31) Grimme, S.; Ehrlich, S.; Goerigk, L. Effect of the damping function in dispersion corrected density functional theory. *J. Comput. Chem.* **2011**, *32* (7), 1456−1465.
(32) Hay, P. J.; Wadt, W. R. Ab initio effective core potentials for molecular calculations. Potentials for the transition metal atoms Sc to Hg. *J. Chem. Phys.* **1985**, *82* (1), 270−283.
(33) Weigend, F. Accurate Coulomb-fitting basis sets for H to Rn. *Phys. Chem. Chem. Phys.* **2006**, *8* (9), 1057−1065.
(34) Francl, M. M.; Pietro, W. J.; Hehre, W. J.; Binkley, J. S.; Gordon, M. S.; DeFrees, D. J.; Pople, J. A. Self-consistent molecular orbital methods. XXIII. A polarization-type basis set for second-row elements. *J. Chem. Phys.* **1982**, *77* (7), 3654−3665.
(35) Hariharan, P. C.; Pople, J. A. The influence of polarization functions on molecular orbital hydrogenation energies. *Theor. Chim. Acta* **1973**, *28* (3), 213−222.
(36) Luchini, G.; Alegre-Requena, J.; Funes-Ardoiz, I.; Paton, R. GoodVibes: automated thermochemistry for heterogeneous computational chemistry data [version 1; peer review: 2 approved with reservations]. *F1000Research* **2020**, *9*, 291.
(37) Grimme, S. Supramolecular Binding Thermodynamics by Dispersion-Corrected Density Functional Theory. *Chem.—Eur. J.* **2012**, *18* (32), 9955−9964.
(38) Li, Y.-P.; Gomes, J.; Mallikarjun Sharada, S.; Bell, A. T.; Head-Gordon, M. Improved Force-Field Parameters for QM/MM Simulations of the Energies of Adsorption for Molecules in Zeolites and a Free Rotor Correction to the Rigid Rotor Harmonic Oscillator Model for Adsorption Enthalpies. *J. Phys. Chem. C* **2015**, *119* (4), 1840−1850.
(39) Krishnan, R.; Binkley, J. S.; Seeger, R.; Pople, J. A. Self-consistent molecular orbital methods. XX. A basis set for correlated wave functions. *J. Chem. Phys.* **1980**, *72* (1), 650−654.
(40) McLean, A. D.; Chandler, G. S. Contracted Gaussian basis sets for molecular calculations. I. Second row atoms, Z = 11−18. *J. Chem. Phys.* **1980**, *72* (10), 5639−5648.
(41) Tomasi, J.; Mennucci, B.; Cammi, R. Quantum Mechanical Continuum Solvation Models. *Chem. Rev.* **2005**, *105* (8), 2999−3094.
(42) Hopmann, K. H. How Accurate is DFT for Iridium-Mediated Chemistry? *Organometallics* **2016**, *35* (22), 3795−3807.
(43) *GaussView Version 6.0.16*; Semichem, Inc.: Shawnee Mission, KS, 2019. (Accessed July 17, 2024.)
(44) Bhattacharyya, D.; Videla, P. E.; Cattaneo, M.; Batista, V. S.; Lian, T.; Kubiak, C. P. Vibrational Stark shift spectroscopy of catalysts under the influence of electric fields at electrode−solution interfaces. *Chem. Sci.* **2021**, *12* (30), 10131−10149.
(45) Clark, M. L.; Ge, A.; Videla, P. E.; Rudshteyn, B.; Miller, C. J.; Song, J.; Batista, V. S.; Lian, T.; Kubiak, C. P. CO_2 Reduction Catalysts on Gold Electrode Surfaces Influenced by Large Electric Fields. *J. Am. Chem. Soc.* **2018**, *140* (50), 17643−17655.
(46) Sarkar, S.; Patrow, J. G.; Voegtle, M. J.; Pennathur, A. K.; Dawlaty, J. M. Electrodes as Polarizing Functional Groups: Correlation between Hammett Parameters and Electrochemical Polarization. *J. Phys. Chem. C* **2019**, *123* (8), 4926−4937.